SEARCHING FOR THE OPTIMAL CURVELET TILING

Hasan Al-Marzouqi and Ghassan AlRegib

School of Electrical and Computer Engineering
Georgia Institute of Technology, Atlanta, GA, 30332-0250
{almarzouqi,alregib}@gatech.edu

ABSTRACT

Curvelets were recently introduced as a popular extension of wavelets. In the curvelet domain the input image is represented by sets of coefficients representing signal energy in different scales and angular directions. In this paper an algorithm that searches for optimal tilings for use with the curvelet transform is introduced. We consider two adaptations: scale locations, and the number of angular divisions per scale. A search algorithm that searches for the optimal tiling with respect to denoising performance is introduced. Results show significant improvement over original curvelet tilings. Tiling results were also tested with a seismic compressed sensing recovery problem. A similar performance advantage is reported.

Index Terms— image processing, curvelet transform, denoising, seismic recovery, wavelet extension

1. INTRODUCTION

The curvelet transform [1] decomposes an image into a representation that emphasizes its directional characteristics across different scales. This is accomplished through dyadic division of input data's frequency content using a pseudo-polar tiling (Figure 1). This division allows for efficient directional representation of edges. The polar version of this tiling is shown to be optimal [2], in terms of partial reconstruction error, for representing objects that are smooth except for discontinuities along C^2 curves, which have continuous first and second derivatives. The transform has been used in a wide variety of image processing applications. Examples include: image denoising and speckle reduction [3, 4], image fusion [5], and contrast enhancement [6]. In this paper, we consider adapting the default curvelet tiling. The location of scales and the number of angular divisors per scale is going to be optimized with respect to a cost function chosen to indicate the performance of a curvelet based denoising algorithm. The cost function used in this work is the reduction in mean squared error (MSE) obtained from denoising images corrupted with additive white gaussian noise(AWGN).

The remainder of the paper is organized as follows. In the next section, a technical overview of the curvelet transform is presented. Section 3 discusses adaptation details and introduces the optimization algorithm. Denoising and compressed sensing recovery results are shown in section 5.

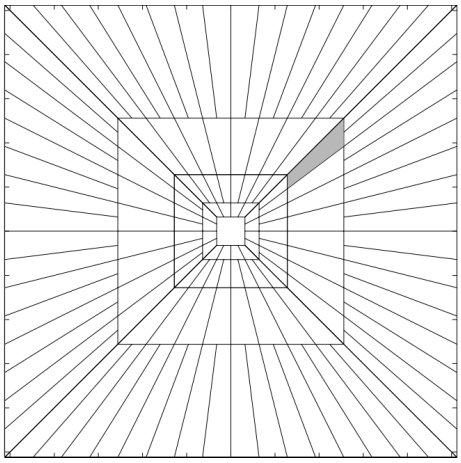

Fig. 1. Default curvelet tiling[1]

2. THE CURVELET TRANSFORM

The transform starts by taking the 2D FFT of the given input image. Next, the FFT is divided into tiles as shown in Fig. 1. Notice that the inner most level is not directional. Periodic extension is used in the outer scale. This is necessary since the FFT implicitly assumes that the left/upper most pixel and the right/lower most pixel are immediate neighbors. To prevent discontinuities and high magnitude coefficient values, each wedge is multiplied by complementary smoothing functions U_1 and U_2 around each of its four edges (Fig. 2). Each pixel value p in the smoothing region between two wedges is multiplied by U_1 and U_2. pU_1 will be stored with the coefficients representing the first wedge. Similarly, pU_2 will be stored with the coefficients representing the second wedge.

Perfect recovery from the coefficients is made possible by ensuring that the smoothing functions are normalized so that the following property holds:

$$U_1^2 + U_2^2 = 1 \tag{1}$$

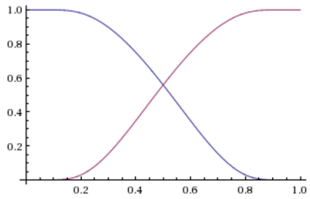

Fig. 2. The two smoothing functions U_1 and U_2.

Curvelet coefficients are the invese FFT of each smoothed wedge. Taking the inverse FFT on these non-rectangular wedges can be performed by a "wrapping" operation. In this step every wedge is localized inside a parallelogram (Fig. 3). Using the periodicity of FFT, the space is tiled with copies of this parallelogram. The inverse FFT is then taken on the rectangle surrounding the origin with the parallelogram's length and height. Mathematically a curvelet coefficient at scale *j*, angular division *l*, and location *k*={*k1,k2*} is described by:

$$c(j,l,k) = \frac{1}{N^2} \sum_{n_1=1}^{L_1} \sum_{n_2=1}^{L_2} W(U_{j,l} f)[n1,n2] e^{2\pi i (k_1 n_1 / L_1 + k_2 n_2 / L_2)} \quad (2)$$

Where *W* is the wrapping function, $U_{j,l}$ is the smoothing window built for wedge (*j,l*). L_1 and L_2 are the horizontal and vertical number of pixels in wedge (*j,l*). *N* is the number of pixels in image *f*. The inverse curvelet transform works by "reversing" forward transform operations.

3. ADAPTING CURVELET TILINGS

3.1. Number of decomposition scales

A scale selection algorithm for selecting the optimal number of scales was introduced in [7]. The algorithm modifies the default curvelet choice of the number of scales *J*. It ensures that the centered high frequency region that is typically seen in many images is part of the inner curvelet scale and is not being smoothed by angular divisions. The optimal number of scales given by the scale selection algorithm is

$$J = \lceil \log_2 (\frac{\min(N1, N2)}{D}) \rceil \quad (3)$$

Where *D* is the length of the square covering the high frequency magnitude values. *N1* and *N2* are the number of horizontal and vertical image pixels respectively. The default curvelet choice for the number of decomposition levels is given by:

$$J = \lceil \log_2 (\min(N1, N2) - 3) \rceil \quad (4)$$

3.2. Optimal number of divisions per quadrant/scale

The optimal number of divisions per scale is found by testing denoising performance while varying the number of wedges per quadrant. The number of possible parameter choices is 2(*J*-1) for real data and is 4(*J*-1) for complex data. Each one of these parameters is varied in steps of four from 4 to the maximum desired number of divisions. This independent optimization is possible, since performance for each quadrant/scale pair is local to its region of support. The algorithm returns the parameter values associated with the best denoising performance.

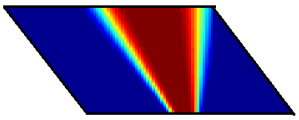

Fig. 3. Smoothing functions localized on a wedge are shown with the wedge's parallelogram shaped support region. Function values decrease from 1 to 0 as we move from red to blue.

3.3. Scale locations

Curvelets divide the FFT plane into scales using a non-adaptive dyadic manner. In this section a search algorithm is introduced that searches for the optimal scale locations. This also includes searching for the optimal periodic extension size that is used for the outer level curvelets. Searching for the optimal scale locations was done using the Nelder-Mead simplex method [8]. The parameters to be optimized are distances to the image center. Scales are not restricted to be of equal height and length. The number of optimizing parameters is therefore 2*J*. Constraints were enforced using a function that would return a very high MSE value if a violation instance was observed. This function will also round parameter values requested by the Nelder-Mead method to the nearest integer. The enforced constraints are:

1. Outer extension level *J* is outside the image boundaries.
2. Level *J*-1 is inside the image boundaries.
3. A minimum number of pixels exists between neighboring scales.
4. A minimum number of pixels exists between the inner scale and image center.
5. Scale distances to the origin increase as scale number increases.

3.4. The global optimization algorithm

A global algorithm combining the previous adaptations is shown in Fig. 4. It uses a multi-resolution search strategy. The algorithm starts with selection of the appropriate number of scale decompositions *J*. Optimization is done in a hierarchical manner consisting of *n* loops. In each loop optimal angular and scale locations are found for a downsampled smoothed version of the image. Angular divisions algorithm

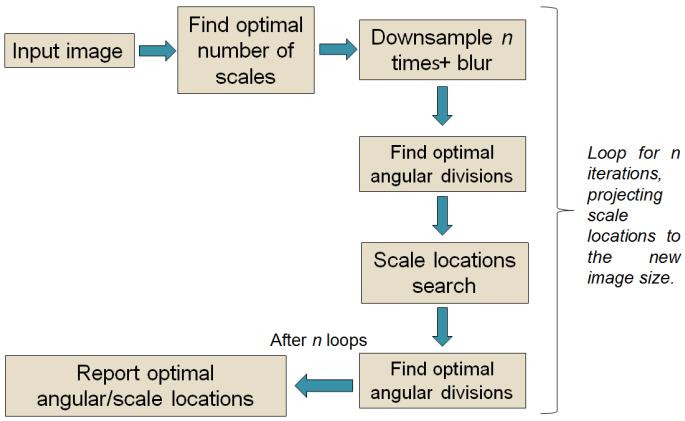

Fig. 4. The global optimization algorithm

runs once with default scale locations before scale location search. These angular optimal values are used in the scale locations search algorithm. Seed values for the scale locations algorithm in the first iteration are the default scale locations corresponding the n^{th} loop image size. Next, angular division search is performed using the computed optimal scale locations. After each round, the observed optimal scale locations are used as a seed for the next iteration. These locations are rescaled to correspond to the new image size.

4. RESULTS

The developed algorithm was tested on a seismic data set. Training data used were $K = 25$ collections of seismic traces. Each collection is of size 550×100 pixels. The curvelet transform is optimized using this training set. The cost function is denoising performance as measured by Mean Squared Error (MSE). The optimal scale locations are found by rounding the average *K* optimal results to the nearest integer. Similarly, optimal angular divisions were found by averaging the *K* optimal divisions and rounding to the nearest even integer. In the next section the thresholding based denoising algorithm is described along with results showing denoising improvements.

4.1. Denoising

The denoising algorithm used in this work [3] applies a simple monte-carlo simulation to estimate wedge noise standard deviation from the estimate of the noise standard deviation σ corrupting the original image. The local noise level for wedge$_{j,l}$ $\sigma_{j,l}$ coming from a scale decomposition S_{opt} and angular decomposition A_{opt} is estimated by applying the curvelet transform with the same scale and angular decomposition to a white noise image with σ noise level. The wedge dependant noise standard deviation is computed using the generated coefficients. This local noise estimation is repeated for few more iterations to reach a reliable estimate. Let $\widehat{c}$ be

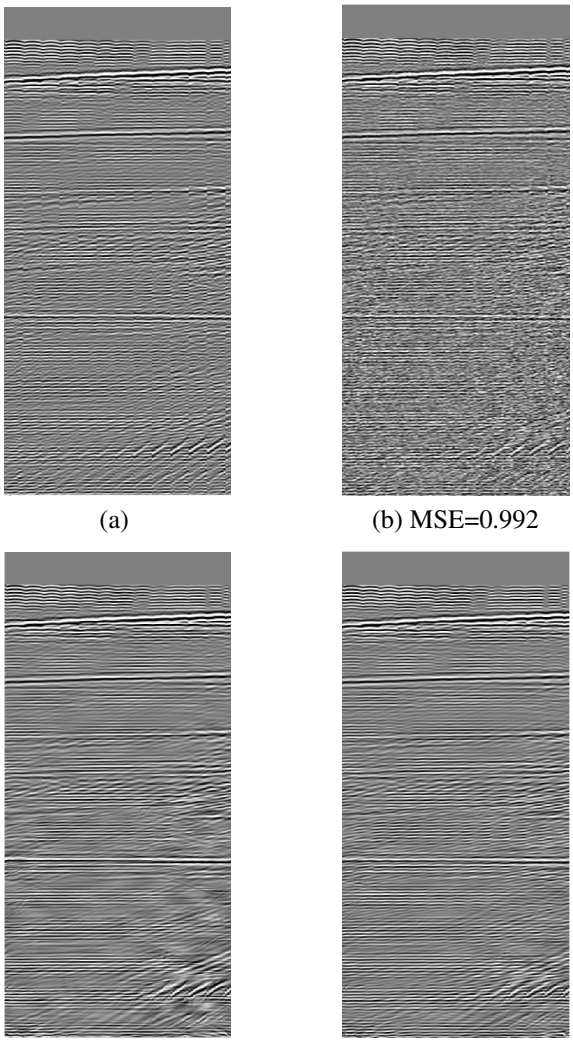

(a) (b) MSE=0.992

(c) MSE=0.852 (d) MSE=0.524

Fig. 5. Denoising results (a)-(b) Original and noisy images, (c) Curvelet denoising (d) Adaptive curvelet denoising

the noisy curvelet coefficients. Restored image coefficients c are given by hard-thresholding according to:

$$c = \widehat{c} \qquad \text{if } |\widehat{c}| \geq k\sigma_{j,l} \tag{5}$$

$$c = 0 \qquad \text{if } |\widehat{c}| < k\sigma_{j,l} \tag{6}$$

Where $k = 4$ for the outer scale, and is equal to three otherwise. Optimal tilings found were applied to to testing data and denoising results were compared with the original curvelet algorithm. Results show considerable quantitative and visual improvement (Fig. 5).

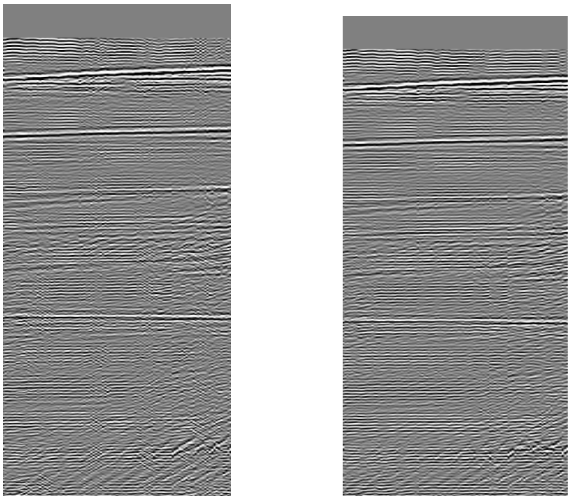

(a) MSE=3.282 (b) MSE=1.316

Fig. 6. Recovery of seismic data Fig 5(a) using $\delta = 0.5$ (a) Using default curvelets (b) Using adaptive tilings

4.2. Recovery from incomplete data

Recent results in compressed sensing theory allows for data reconstruction from a lower number of samples. This has been exploited in seismic exploration with the aid of curvelets to obtain more information content from less number of measurements [9]. The success of adaptive tiling curvelets with denoising can be related to a better concentration of signal energy into a small number of coefficients. Therefore, it is reasonable to assume that better CS based recovery is possible using the optimal denoising tiles. Experimental results summarized below verified this assumption.

Assume that the data collected are in the form of vector $\mathbf{b} = S\mathbf{f} \in R^n$. Where $\mathbf{f} \in R^N$ is the vector of complete data points. S is the sampling matrix that randomly samples $\delta = \frac{n}{N}$ seismic traces. Let $C^{-1}(\mathbf{x})$ be the inverse curvelet transform of $\mathbf{x}$. The vector of complete measurements $\mathbf{f}$ can be approximated by solving the following program:

$$\hat{\mathbf{f}} = C^{-1}(\hat{\mathbf{x}}) \quad \text{with } \hat{\mathbf{x}} = \arg_{\mathbf{x}} \min \|\mathbf{x}\|_1 \text{ subject to } SC^{-1}(\mathbf{x}) = \mathbf{b} \tag{7}$$

Numerous algorithms are available that solve the above optimization problem. The Spectral Projected Gradient algorithm (SPGL1) is used in this study [10]. The recovery algorithm was tested using a sampling ratio of $\delta = 0.5$. An example showing the improvements in the recovery process due to adaptive tiling is shown in Fig. 6.

5. CONCLUSIONS

Algorithms for adapting and searching for optimal curvelet tilings were introduced in this work. The toolkit allows for customizing curvelet tilings based on a collection of input images representing a specific class of data. The algorithm was shown to succeed in improving curvelet results in seismic denoising and seismic data recovery. Similar performance improvements are expected in other application areas. The adaptive tiling approach taken in this study can also be extended to other *curvelet-like* transforms such as *shearlets* [11], and *contourlets* [12]. Deciding on the optimal curvelet tilings based on an individual image FFT content remains an interesting open problem.

6. REFERENCES

[1] Candes, E. and Demanet, L. and Donoho, D. and Ying, L., "Fast discrete curvelet transforms," *Multiscale Modeling & Simulation*, vol. 5, no. 3, pp. 861–899, 2006.

[2] Candes, E.J. and Donoho, D.L., "New tight frames of curvelets and optimal representations of objects with piecewise c2 singularities," *Communications on pure and applied mathematics*, vol. 57, no. 2, pp. 219–266, 2003.

[3] Starck, J.L. and Candès, E.J. and Donoho, D.L., "The curvelet transform for image denoising," *Image Processing, IEEE Transactions on*, vol. 11, no. 6, pp. 670–684, 2002.

[4] Saevarsson, B.B. and Sveinsson, J.R. and Benediktsson, J.A., "Combined wavelet and curvelet denoising of sar images," in *Geoscience and Remote Sensing Symposium, 2004. IGARSS'04. Proceedings. 2004 IEEE International*. IEEE, vol., pp., 4235–4238.

[5] Choi, M. and Kim, R.Y. and Nam, M.R. and Kim, H.O., "Fusion of multispectral and panchromatic satellite images using the curvelet transform," *Geoscience and remote sensing letters, IEEE*, vol. 2, no. 2, pp. 136–140, 2005.

[6] Miri, M.S. and Mahloojifar, A., "Retinal image analysis using curvelet transform and multistructure elements morphology by reconstruction," *Biomedical Engineering, IEEE Transactions on*, vol. 58, no. 5, pp. 1183–1192, 2011.

[7] Al-Marzouqi, H. and AlRegib, G., "Curvelet transform with adaptive tiling," in *IS&T/SPIE Electronic Imaging*. International Society for Optics and Photonics, pp., 82950F–82950F.

[8] Avriel, M., *Nonlinear programming: analysis and methods*, Dover Publications, 2003.

[9] Herrmann, F.J. and Hennenfent, G., "Non-parametric seismic data recovery with curvelet frames," *Geophysical Journal International*, vol. 173, no. 1, pp. 233–248, 2008.

[10] van den Berg, E. and Friedlander, MP, "Spgl1: A solver for large-scale sparse reconstruction," *Online: http://www.cs. ubc. ca/labs/scl/spgl1*, 2007.

[11] Guo, K. and Labate, D., "Optimally sparse multidimensional representation using shearlets," *SIAM journal on mathematical analysis*, vol. 39, no. 1, pp. 298–318, 2007.

[12] Do, M.N. and Vetterli, M., "The contourlet transform: an efficient directional multiresolution image representation," *Image Processing, IEEE Transactions on*, vol. 14, no. 12, pp. 2091–2106, 2005.